

# An Accurate Lubrication Model of Contaminated Coating Flows

A.J. Roberts & M.E. Simpson\*

*Department of Mathematics and Computing, University of  
Southern Queensland, Toowoomba, Australia*

March 6, 2022

## Abstract

The levelling of short-wave irregularities on a thin film of fluid is primarily due to the action of surface tension. Surface tension gradients are often created by a number of different factor including evaporation, thermal gradients or deposition of surfactants. Lubrication theory, which ignores inertia terms in favour of viscous terms, produces a system of two nonlinear PDE's for the unsteady flow of a thin viscous Newtonian fluid containing an insoluble surfactant. A complex model, which systematically includes all relevant effects to these PDE's, is developed using centre manifold techniques. The benefits of using these techniques to develop accurate models are in their application. Subtle variations in parameters or assumptions are able to be catered for by including or deleting the relevant terms rather than having to redevelop these models. Computed solutions of both models using the same numerical process are compared. Numerical simulations also demonstrate the long-term stabilisation of corrugations by induced surfactant variations.

**Keywords:** surfactant, centre manifold, low-dimensional modelling.

## Contents

### 1 Introduction

2

---

\*mailto:aroberts@usq.edu.au, simpsonm@usq.edu.au

<b>1</b>	<b>INTRODUCTION</b>	<b>2</b>
<b>2</b>	<b>Mathematics models the physical processes</b>	<b>4</b>
<b>3</b>	<b>The basis of the centre manifold analysis</b>	<b>6</b>
<b>4</b>	<b>The centre manifold model</b>	<b>8</b>
<b>5</b>	<b>Stability analysis of simple flows</b>	<b>10</b>
<b>6</b>	<b>Numerical simulations</b>	<b>12</b>
<b>7</b>	<b>Summary</b>	<b>15</b>
<b>A</b>	<b>Computer algebra code</b>	<b>17</b>

## 1 Introduction

Thin film flows are common in a large number of industrial and biological flows. Industrial applications include liquid agrochemicals, production of photographic film, lubricants, adhesives, dyes and surfactants. Biological flows include thin liquid films on the cornea of the eye and on the linings of the lungs. The development of accurate models is therefore essential for a proper understanding of these flows.

The development of models for the evolution of a thin clean film on arbitrarily curved substrates has been well documented over recent years. Levich [15] developed a model for the motion of thin and wide fluid films induced by a surface tension variation. Inconsistencies in the assumptions in Levich's solution were corrected by Yih [23] in 1968. Kennings [14] provided a valuable contribution to the qualitative effects on interfacial motion by surface tension gradients. Ahmad & Hansen [2] considered the spreading of a monolayer over a thin liquid film and argued that the distance spread in time  $t$  is  $x^2 = (2H/\mu)\pi_0 t$  where  $H$  is the liquid-film thickness,  $\mu$  the coefficient of viscosity of the liquid underlying the monolayer and  $\pi_0$  is the spreading pressure of the lens generating the monolayer. This relation was verified in experiments by Hussain, Fatima & Ahmad [13] in 1975.

DiPietro, Huh & Cox [7], DiPietro & Cox [6] and Foda & Cox [8] analysed the spreading of one liquid on the surface of a deep fluid. They provide an extensive overview of the interfacial dynamics associated with the spreading of a contaminant.

These papers used methods to develop models with specific parameter values. If the physics of the problem required the reordering of these parameterised physical processes, then, in traditional approaches all the mod-

elling needs to be performed again. However, modern dynamical systems theory provides systematic methods to derive comprehensive and flexible low-dimensional models of spatio-temporal evolution. Centre manifold theory is one such method used successfully in deriving flexible and accurate models as shown by Roberts in 1996 and 1997 [18, 19]. Roy *et al* [20] also used these techniques to demonstrate the importance of higher order terms in conserving mass.

This work continues on from that analysis by now developing thin fluid film models including effects due to the contamination of the surface with an insoluble surfactant. In addition the effects of inertia and van der Waals forces are included for completeness. The relevant equations, boundary conditions and constitutive equations are analysed in Section 3 using centre manifold theory in order to generate the low-dimensional model for the dynamics. In Section 4 these equations are solved using the computer algebra package REDUCE to compute evolution equations for the given problem to any order required. The evolution equations to low order are

$$\begin{aligned}
\frac{\partial \eta}{\partial t} &= -\frac{1}{2} \frac{\partial}{\partial x} (\eta^2 \gamma_x) - \frac{1}{3} \frac{\partial}{\partial x} (\eta^3 (\gamma \eta_{xx})_x) \\
&\quad - \frac{1}{3} \frac{\partial}{\partial x} (\eta^3) \mathcal{B} \sin \theta + \frac{1}{3} \frac{\partial}{\partial x} (\eta^3 \eta_x) \mathcal{B} \cos \theta - \frac{\partial}{\partial x} \left( \frac{\eta_x}{\eta} \right) \mathcal{H} \\
&\quad + \mathcal{O}(\partial_x^6 + \mathcal{B}^2 + \mathcal{H}^2) \quad \text{and} \tag{1} \\
\frac{\partial \Gamma}{\partial t} &= -\frac{\partial}{\partial x} (\Gamma \eta \gamma_x) - \frac{1}{2} \frac{\partial}{\partial x} (\Gamma \eta^2 (\gamma \eta_{xx})_x) \\
&\quad - \frac{1}{2} \frac{\partial}{\partial x} (\Gamma \eta^2) \mathcal{B} \sin \theta + \frac{1}{2} \frac{\partial}{\partial x} (\Gamma \eta^2 \eta_x) \mathcal{B} \cos \theta - \frac{3}{2} \frac{\partial}{\partial x} \left( \frac{\Gamma \eta_x}{\eta^2} \right) \mathcal{H} \\
&\quad + \frac{\delta_s}{\sqrt{1 + \eta_x^2}} \frac{\partial}{\partial x} \left( \frac{\Gamma_x}{1 + \eta_x^2} \right) \\
&\quad + \mathcal{O}(\partial_x^6 + \mathcal{B}^2 + \mathcal{H}^2) \tag{2}
\end{aligned}$$

where  $\mathcal{B}$ ,  $\mathcal{H}$  and  $\delta_s$  is a Bond number, a Hamaker constant and an inverse Péclet number respectively. We have reproduced the evolution models of Gaver and Grotberg [10], de Wit [4] and others except for the additional term in the evolution equation of the contaminant which reflects the importance of gradient effects. However, in Section 4 we show that these models do not capture all the terms required for accuracy. The relevance of these terms will become apparent in the physics of the problem.

The comprehensive structurally stable model 1–2 which is compared numerically in Section 7 to a number of similar models developed recently [4, 10, 21] using traditional lubrication methods. These simulations show that

our model better captures the effects of steep gradients. This is expected as only our model includes this term which demonstrates the flexibility of our approach, which rests on the Approximation Theorem [3], when analysing flows with parameters in a different physical region. Inappropriate terms are simply deleted from the comprehensive model rather than having to redevelop a new model using the new assumptions.

Finally numerical simulations of examples shown in Section 6 confirm the long-lasting corrugations predicted by the linear analysis in Section 5. These corrugations only decay by the very slow diffusion of surfactant.

## 2 Mathematics models the physical processes

Consider a thin film of fluid of varying thickness  $\eta(x, t)$  lying on a flat substrate. An orthogonal coordinate system  $(x, y)$  is used where  $x$  measures distance along the substrate located at  $y = 0$ . The surface of the fluid is thus described by  $y = \eta(x, t)$ . The incompressible Newtonian fluid of viscosity  $\mu$  and density  $\rho$ , undergoes slow creeping flow. The dynamics of the fluid flow are determined by pressure gradients caused by surface tension forces which in turn are affected by the surfactant concentration. The equations of motion to be solved are the continuity and Navier-Stokes equations together with boundary conditions. For convenience we non-dimensionalise by scaling variables with respect to: a typical film thickness  $H$ , a reference value of the surfactant concentration  $\Gamma_0$  and surface tension  $\gamma_0$  at  $\Gamma = \Gamma_0$ , the reference time  $\mu H / \gamma_0$ , the reference velocity  $U = \gamma_0 / \mu$ , and the reference pressure  $\gamma_0 / H$ . The equations of motion then are written

$$\nabla \cdot \mathbf{q} = 0 \quad \text{and} \quad (3)$$

$$\mathcal{R} \left[ \frac{\partial \mathbf{q}}{\partial t} + \mathbf{q} \cdot \nabla \mathbf{q} \right] = -\nabla(p + W) + \nabla^2 \mathbf{q} + \mathcal{B} \mathbf{g}, \quad (4)$$

where  $\mathcal{R} = \gamma_0 \rho H / \mu^2$  is a Reynolds number,  $\mathcal{B} = \rho g H^2 / \gamma_0$  is a Bond number,  $W = \mathcal{H} / \eta^3$  is the simple model of the van der Waals force used by de Wit *et al* [4] and described in detail by Maldarelli *et al* [16] in which  $\mathcal{H} = H_a \rho / H \mu^2$  is a nondimensional Hamaker constant where  $H_a = 10^{-12}$  erg is a typical value of the dimensional Hamaker constant,  $\mathbf{q}(x, y, t)$  is the fluid velocity,  $p(x, y, t)$  is the pressure field and  $\mathbf{g}$  is the direction of gravitational normal force at an angle  $\theta$  to the substrate ( $\theta = \pi/2$  is draining flow and  $\theta = \pi$  generally leads to dripping). These equations are to be solved with the following boundary conditions:  $\mathbf{q} = \mathbf{0}$  on the substrate  $y = 0$ ; the normal stress on the free surface must balance normal surface tension, that is,

$$p = \tilde{\boldsymbol{\tau}}_{\mathbf{n}} \cdot \tilde{\mathbf{n}} - \gamma \tilde{\kappa} \quad \text{on } y = \eta, \quad (5)$$

where  $\tilde{\boldsymbol{\tau}}_n$  is the deviatoric stress across the surface,  $\tilde{\kappa}$  is the mean curvature of the free surface,  $\tilde{\boldsymbol{n}}$  is a unit normal to the free surface,  $\gamma$  is the local value of the surface tension and a tilde indicates evaluation at the free surface; tangential stress on the free surface must equal the surface tension gradients, that is,

$$\tilde{\boldsymbol{\tau}}_n \cdot \tilde{\boldsymbol{t}} = \tilde{\boldsymbol{t}} \cdot \nabla \gamma \quad \text{on } y = \eta, \quad (6)$$

where  $\tilde{\boldsymbol{t}}$  is a unit tangent to the free surface; and the kinematic condition

$$\frac{\partial \eta}{\partial t} = \tilde{v} - \tilde{u} \frac{\partial \eta}{\partial x} \quad (7)$$

states that the fluid particles on the free surface must follow the free surface.

The dynamics of a surfactant on the fluid surface is described by a PDE which we derive here using conservation arguments. Consider an arbitrary interval of substrate,  $x$  in  $I = [a, b]$ , and the fluid above it. Let the fluid surface have a concentration of surfactant per unit area of the fluid surface,  $\Gamma_0 \Gamma(x, t)$  where  $\Gamma_0$  is a typical value for the concentration and  $\Gamma(x, t)$  gives the nondimensional variations. Thus the nondimensional surface concentration per unit area of substrate is  $\sqrt{1 + \eta_x^2} \Gamma$ . Conservation of mass implies that the rate of change of surfactant mass in  $I$  is equal to the rate of mass influx across the ends. The rate of change of mass of surfactant in  $I$  is

$$\frac{d}{dt} \int_I \left[ \Gamma \sqrt{1 + \eta_x^2} \right] dx = \int_I \left[ \sqrt{1 + \eta_x^2} \frac{\partial \Gamma}{\partial t} + \Gamma \frac{\partial}{\partial t} \sqrt{1 + \eta_x^2} \right] dx \quad (8)$$

$$= \int_I \left[ \sqrt{1 + \eta_x^2} \frac{\partial \Gamma}{\partial t} + \Gamma \frac{\eta_x \eta_{xt}}{\sqrt{1 + \eta_x^2}} \right] dx. \quad (9)$$

The fluid on the free surface, lateral velocity  $\tilde{u}$ , carries the surfactant to produce a flux parallel to the substrate (in the  $x$ -direction) of

$$\tilde{u} \Gamma \sqrt{1 + \eta_x^2}. \quad (10)$$

Molecular diffusion of surfactant on the free surface carries a flux

$$\frac{D_s}{\sqrt{1 + \eta_x^2}} \frac{\partial \Gamma}{\partial s} = \frac{D_s}{(1 + \eta_x^2)} \frac{\partial \Gamma}{\partial x} \quad (11)$$

where  $D_s$  is a surface diffusivity coefficient. The additional geometric term,  $1/\sqrt{1 + \eta_x^2}$ , appears because although the flux on the surface is  $D_s \frac{\partial \Gamma}{\partial s}$  the direction of the flux is at an angle to the substrate and requires multiplication

by the direction cosine  $1/\sqrt{1+\eta_x^2}$ . The net rate of gain of surfactant in the interval  $I$  through these transport mechanisms is

$$\left[ \Gamma \tilde{u} \sqrt{1+\eta_x^2} - \frac{D_s}{(1+\eta_x^2)} \frac{\partial \Gamma}{\partial x} \right] \Big|_a^b = \int_I \frac{\partial}{\partial x} \left[ \Gamma \tilde{u} \sqrt{1+\eta_x^2} - \frac{D_s}{(1+\eta_x^2)} \frac{\partial \Gamma}{\partial x} \right] dx. \quad (12)$$

Equating (9) to (12) using (7) and after some algebraic manipulation, we obtain (noting  $\tilde{u}_x$  is  $\frac{\partial}{\partial x}(\tilde{u})$ , not  $\frac{\partial u}{\partial x}|_{y=\eta}$ , and similarly for  $\tilde{v}_x$ )

$$\frac{\partial \Gamma}{\partial t} = \frac{\delta_s}{\sqrt{1+\eta_x^2}} \frac{\partial}{\partial x} \left[ \frac{\Gamma_x}{(1+\eta_x^2)} \right] - \frac{\partial}{\partial x} (\Gamma \tilde{u}) + \frac{\Gamma \tilde{u}_x \eta_x^2 - \Gamma \tilde{v}_x \eta_x}{(1+\eta_x^2)}, \quad (13)$$

where  $\delta_s = 1/\mathcal{P} = D_s \mu / \gamma_0 H$  is an inverse Péclet number characterising the importance of surface diffusion compared with advection.

To obtain a well-posed problem a further equation is needed relating surface tension,  $\gamma$ , and surfactant concentration,  $\Gamma$ . It is well established [1, 15, 22, e.g.] that the surface tension is a function of the surface concentration,  $\gamma = \gamma(\Gamma)$ . Here we chose to use a linear relationship between surface tension and surfactant concentration following Schwartz *et al* [21] namely,

$$\gamma = 1 + A(1 - \Gamma), \quad (14)$$

where  $\gamma$  has been nondimensionalised by scaling with respect to the reference value of the surface tension  $\gamma_0$  at  $\Gamma = \Gamma_0$  and

$$A = \frac{\Gamma_0}{\gamma_0} \frac{\partial \gamma}{\partial \Gamma}. \quad (15)$$

### 3 The basis of the centre manifold analysis

In this section we lay the basis for forming an accurate model of the dynamics of the thin fluid film with surfactant. We adapt the governing fluid equations (3–4), the surfactant evolution equation (13), the relevant boundary conditions (5–7) and the constituent equation (14) to a form suitable for the application of centre manifold theory and techniques in order to generate a low-dimensional model for the dynamics.

We develop a model of slow large scale flow by invoking the slowly varying assumption, that is  $\partial/\partial x$  is small, and with weak forcing, that is  $\mathcal{B}$  and  $\mathcal{H}$  are also small. In centre manifold theory this is achieved by treating  $\partial/\partial x$ ,  $\mathcal{B}$  and  $\mathcal{H}$  terms as “nonlinear” perturbations. Thus the linear picture is obtained by neglecting any  $\partial/\partial x$ ,  $\mathcal{B}$  and  $\mathcal{H}$  terms. This may be seen as being equivalent to the multiple-scale assumption of variations occurring only on

a large lateral length scale (see Roberts [17, 18, 19] for a fuller explanation). We also assume that the fluid is thin enough for gravity to be a perturbing influence but thick enough for van der Waals forces to also be a perturbing influence, that is, the Bond and Hamaker numbers are both small.

The “linear” dynamics are then solutions of the following equations

$$\frac{\partial v}{\partial y} = 0, \quad (16)$$

$$\mathcal{R} \frac{\partial \mathbf{q}}{\partial t} + \frac{\partial p}{\partial y} \mathbf{j} - \frac{\partial^2 \mathbf{q}}{\partial y^2} = 0, \quad (17)$$

$$\frac{\partial \Gamma}{\partial t} = 0, \quad (18)$$

with boundary conditions

$$\mathbf{q} = \mathbf{0} \quad \text{on } y = 0, \quad (19)$$

$$-p + 2 \frac{\partial v}{\partial y} = 0 \quad \text{on } y = \eta, \quad (20)$$

$$\frac{\partial u}{\partial y} + \frac{\partial v}{\partial x} = 0 \quad \text{on } y = \eta, \quad (21)$$

$$\frac{\partial \eta}{\partial t} - v = 0 \quad \text{on } y = \eta, \quad (22)$$

All solutions of these linear equations are composed of the decaying lateral shear modes  $v = p = 0, u = b \sin(l\pi y/(2\eta)) \exp(\lambda_l t)$ , together with two critical modes  $\eta = \text{constant}$  and  $\Gamma = \text{constant}$ . Here the integer  $l$  parameterises the vertical wavenumber and the decay rate of the lateral shear modes are  $-\lambda_l = l^2 \pi^2 / (4\eta^2 \mathcal{R})$ . So linearly, and in the absence of any lateral variations on a flat substrate, all the lateral shear modes decay exponentially quickly, on a time-scale of  $\mathcal{R}\eta^2$ , just leaving a film of constant thickness with a covering of surfactant of constant concentration as the permanent mode. This spectrum, of all eigenvalues strictly negative except for a few that are zero, is the classic spectrum for the application of centre manifold theory: the Existence Theorem in [3] assures that the nonlinear effects in the physical equations just perturb this linear picture of the dynamics so that in the long-term all solutions of the full nonlinear system are dominated by the slow dynamics induced by nonlinearities and large-scale lateral variations in the film thickness and contaminant. The Relevance Theorem in [3] assures that these dynamics are exponentially attractive, asymptotically complete, and so form a generic model of the long-term dynamics of the contaminated film. With the caveat that a strict theory has not yet been developed to cover this application to non-linear large-scale flows, the closest being that of Gally [9]

and Hărăgus [12] (but also see [17]), the centre manifold concepts and techniques are applied to systematically develop a low-dimensional lubrication model of the dynamics of the film.

Having identified the critical modes associated with the zero decay-rate, the subsequent analysis is straightforward. The usual approach is to write the fluid fields  $\mathbf{q}(x, y, t) = (u, v)$  and  $p(x, y, t)$ , as a function of the critical modes  $\eta$  and  $\Gamma$  (equivalent to the “slaving” principle of synergetics [11]). Instead of seeking *explicit* asymptotic expansions in the “amplitudes” of the critical modes [17, 18], an iterative algorithm is applied to find the centre manifold and the evolution thereon which is based directly upon the Approximation Theorem in [3, 19] and its variants; explained in detail by Roberts in [19].

## 4 The centre manifold model

We solve the continuity and Navier-Stokes equations under the assumptions introduced above by programming the computer algebra package REDUCE. The program listed in the Appendix iteratively solves the physical equations using techniques explained by Roberts [17, 19]. We express the velocity and pressure fields in terms of the scaled normal coordinate  $\zeta = y/\eta(x, t)$  to simplify the expressions; in this stretched coordinate the free surface is  $\zeta = 1$ . The computer algebra gives the fluid fields to be

$$\begin{aligned}
u \approx & \left(\zeta - \frac{1}{2}\zeta\right) \mathcal{B} \sin \theta \eta^2 + \left(3\zeta - \frac{3}{2}\zeta^2\right) \mathcal{H} \frac{\eta_x}{\eta^2} \\
& - \left(\zeta - \frac{1}{2}\zeta^2\right) \mathcal{B} \cos \theta \eta^2 \eta_x + \left(\frac{5}{2}\zeta - \frac{1}{2}\zeta^2 - \frac{1}{3}\zeta^3\right) \mathcal{B} \sin \theta \eta^3 \eta_{xx} \\
& + \left(\zeta - \frac{1}{2}\zeta^2\right) \gamma \eta^2 \eta_{xxx} + \zeta \eta \gamma_x, \tag{23}
\end{aligned}$$

$$\begin{aligned}
v \approx & -\frac{1}{2}\zeta^2 \mathcal{B} \sin \theta \eta^2 \eta_x + \left(\frac{9}{2}\zeta^2 - 2\zeta^3\right) \mathcal{H} \frac{\eta_x^2}{\eta^2} + \frac{1}{2}\zeta^2 \mathcal{B} \cos \theta \eta^2 \eta_x^2 \\
& - \left(\frac{3}{2}\zeta^2 - \frac{1}{2}\zeta^3\right) \mathcal{H} \frac{\eta_{xx}}{\eta} + \left(\frac{1}{2}\zeta^2 - \frac{1}{6}\zeta^3\right) \mathcal{B} \cos \theta \eta^3 \eta_{xx} \\
& - \frac{1}{2}\zeta^2 \eta^2 \gamma_{xx} - \frac{5}{2}\zeta^2 \mathcal{B} \sin \theta \eta^2 \eta_x^3 - \left(\frac{15}{2}\zeta^2 - \frac{1}{2}\zeta^3\right) \mathcal{B} \sin \theta \eta^3 \eta_x \eta_{xx} \\
& - \left(\frac{5}{4}\zeta^2 - \frac{1}{6}\zeta^3 - \frac{1}{12}\zeta^4\right) \mathcal{B} \sin \theta \eta^4 \eta_{xxx}, \tag{24}
\end{aligned}$$

$$\begin{aligned}
p \approx & -\gamma \eta_{xx} + (1 - \zeta) \mathcal{B} \cos \theta \eta - (1 + \zeta) \mathcal{B} \sin \theta \eta \eta_x + (1 + \zeta) \mathcal{B} \cos \theta \eta \eta_x^2 \\
& + \left(\frac{1}{2} + \zeta - \frac{1}{2}\zeta^2\right) \mathcal{B} \cos \theta \eta^2 \eta_{xx} + \left(3 + 9\zeta - 6\zeta^2\right) \mathcal{H} \frac{\eta_x^2}{\eta^3}
\end{aligned}$$



$$\begin{aligned}
& - \left( \frac{3}{2} + 3\zeta - \frac{3}{2}\zeta^2 \right) \mathcal{H} \frac{\eta_{xx}}{\eta^2} - (9 + 5\zeta) \mathcal{B} \sin \theta \eta \eta_x^3 \\
& - \left( \frac{27}{2} + 15\zeta - \frac{3}{2}\zeta^2 \right) \mathcal{B} \sin \theta \eta^2 \eta_x \eta_{xx} \\
& - (1 - \Gamma) A \eta_{xx} - 2\eta_x \gamma_x - (1 + \zeta) \eta \gamma_{xx}. \tag{25}
\end{aligned}$$

See that the lateral velocity,  $u$ , is approximately parabolic, Poiseuille flow, which form components of the forcing that act through lateral pressure gradients, but is linear, Couette flow, from the surface tension gradients. Then the velocity normal to the substrate,  $v$ , follows predominately from the continuity equation. These expressions give comprehensive details of the physical fields corresponding to any particular  $\eta(x, t)$  and  $\Gamma(x, t)$ .

The computer algebra also derives the corresponding evolution equations for  $\eta$  and  $\Gamma$  which are

$$\begin{aligned}
\frac{\partial \eta}{\partial t} &= -\frac{1}{2} \frac{\partial}{\partial x} (\eta^2 \gamma_x) - \frac{1}{3} \frac{\partial}{\partial x} (\eta^3 (\gamma \eta_{xx})_x) \\
& - \frac{\partial}{\partial x} \left( \frac{1}{3} \eta^3 + \frac{7}{3} \eta^3 \eta_x^2 + \eta^4 \eta_{xx} \right) \mathcal{B} \sin \theta \\
& + \frac{\partial}{\partial x} \left( \frac{1}{3} \eta^3 \eta_x + \frac{3}{5} \eta^5 \eta_{xxx} + 4\eta^4 \eta_x \eta_{xx} + \frac{7}{3} \eta^3 \eta_x^3 \right) \mathcal{B} \cos \theta \\
& + \frac{\partial}{\partial x} \left( -\frac{\eta_x}{\eta} + \frac{48}{5} \eta_x \eta_{xx} - \frac{9}{5} \eta \eta_{xxx} - 7 \frac{\eta_x^3}{\eta} \right) \mathcal{H} \\
& + \frac{\partial}{\partial x} \left( \frac{32}{105} \eta^2 \eta_x^2 - \frac{10}{21} \eta^3 \eta_{xx} \right) \mathcal{H} \mathcal{R} \mathcal{B} \sin \theta \\
& + \frac{\partial}{\partial x} \left( \frac{44}{105} \eta^3 \eta_x \eta_{xx} + \frac{4}{15} \eta^4 \eta_{xxx} - \frac{4}{105} \eta^2 \eta_x^3 \right) \mathcal{H} \mathcal{R} \mathcal{B} \cos \theta \\
& + \mathcal{O}(\partial_x^6, \mathcal{B}^2, \mathcal{H}^2) \quad \text{and} \tag{26} \\
\frac{\partial \Gamma}{\partial t} &= -\frac{\partial}{\partial x} (\Gamma \eta \gamma_x) - \frac{1}{2} \frac{\partial}{\partial x} (\Gamma \eta^2 (\gamma \eta_{xx})_x) \\
& + \frac{\partial}{\partial x} \left( -\frac{1}{2} \Gamma \eta^2 - \frac{5}{3} \Gamma \eta^3 \eta_{xx} - \frac{17}{4} \Gamma \eta^2 \eta_x^2 \right) \mathcal{B} \sin \theta \\
& + \left( \frac{3}{2} \Gamma \eta \eta_x^3 - \frac{1}{4} \Gamma_x \eta^2 \eta_x^2 \right) \mathcal{B} \sin \theta \\
& + \frac{\partial}{\partial x} \left( \frac{1}{2} \Gamma \eta^2 \eta_x + 4\Gamma \eta^2 \eta_x^3 + \frac{20}{3} \Gamma \eta^3 \eta_x \eta_{xx} + \Gamma \eta^4 \eta_{xxx} \right) \mathcal{B} \cos \theta \\
& + \left( -\Gamma \eta \eta_x^4 + \frac{1}{3} \Gamma \eta^3 \eta_{xx}^2 + \frac{1}{2} \Gamma_x \eta^2 \eta_x^3 + \frac{1}{3} \Gamma_x \eta^3 \eta_x \eta_{xx} \right) \mathcal{B} \cos \theta \\
& + \frac{\partial}{\partial x} \left( -\frac{3}{2} \frac{\Gamma \eta_x}{\eta^2} - \frac{32}{3} \frac{\Gamma \eta_x^3}{\eta^2} + 16 \frac{\Gamma \eta_x \eta_{xx}}{\eta} - 3\Gamma \eta_{xxx} \right) \mathcal{H}
\end{aligned}$$

$$\begin{aligned}
& + \left( -\frac{1}{3} \frac{\Gamma \eta_x^4}{\eta^3} - \frac{\Gamma \eta_{xx}^2}{\eta} + \frac{7}{6} \frac{\Gamma_x \eta_x^3}{\eta^2} - \frac{\Gamma_x \eta_x \eta_{xx}}{\eta} \right) \mathcal{H} \\
& + \frac{\delta_s}{\sqrt{1 + \eta_x^2}} \frac{\partial}{\partial x} \left( \frac{\Gamma_x}{1 + \eta_x^2} \right) \\
& + \frac{\partial}{\partial x} \left( -\frac{89}{120} \Gamma \eta^2 \eta_{xx} + \frac{7}{15} \Gamma \eta \eta_x^2 \right) \mathcal{H} \mathcal{R} \mathcal{B} \sin \theta \\
& + \frac{\partial}{\partial x} \left( \frac{13}{20} \Gamma \eta^2 \eta_x \eta_{xx} + \frac{5}{12} \Gamma \eta^3 \eta_{xxx} - \frac{1}{20} \Gamma \eta \eta_x^3 \right) \mathcal{H} \mathcal{R} \mathcal{B} \cos \theta \\
& + \mathcal{O}(\partial_x^6, \mathcal{B}^2, \mathcal{H}^2). \tag{27}
\end{aligned}$$

The error term  $\mathcal{O}(\partial_x^6, \mathcal{B}^2, \mathcal{H}^2)$  indicates the terms retained in the model by neglecting any term with 6 or more spatial derivatives or any quadratic or higher terms in  $\mathcal{B}$  or  $\mathcal{H}$ . Thus we retain the terms seen above. Any particular application need not retain all of these terms. The Approximation Theorem in [3] supports many consistent truncations of these expressions and the retention of terms is only dependent on the type of application. This model is comprehensively flexible in that it encompasses any model of a similar genre such as those described below.

Gaver and Grotberg [10], de Wit *et al* [4], Schwartz and Weidner [21] and others have previously developed evolution models for this flow using heuristic arguments based on traditional lubrication theory. These models are all similar to the de Wit model:

$$\frac{\partial \eta}{\partial t} \approx -\frac{1}{2} \frac{\partial}{\partial x} (\eta^2 \gamma_x) - \frac{1}{3} \frac{\partial}{\partial x} (\eta^3 (\gamma \eta_{xx})_x) - \mathcal{H} \frac{\partial}{\partial x} \left( \frac{\eta_x}{\eta} \right) \quad \text{and} \tag{28}$$

$$\frac{\partial \Gamma}{\partial t} \approx -\frac{\partial}{\partial x} (\Gamma \gamma_x \eta) - \frac{1}{2} \frac{\partial}{\partial x} (\Gamma \eta^2 (\gamma \eta_{xx})_x) - \frac{3\mathcal{H}}{2} \frac{\partial}{\partial x} \left( \frac{\Gamma \eta_x}{\eta^2} \right) + \delta_s \Gamma_{xx}, \tag{29}$$

and we consider them to be a subset of ours. We have included the effects of gravity (indicated by the Bond number); steeper surface slopes (through  $\sqrt{1 + \eta_x^2}$ ) and the interaction between gravity and van der Waals forces (indicated by  $\mathcal{B}\mathcal{H}$ ) which also involves inertia as the Reynolds number appears. Numerical solutions are compared in §6.

## 5 Stability analysis of simple flows

Linearising the two model's evolution equations (26–27) about a fixed point gives insight into the physical effects taking place. Assume the fluid film is flat with the thickness of the film and the average surfactant concentration both being one in nondimensional units. Then we elucidate the interactive

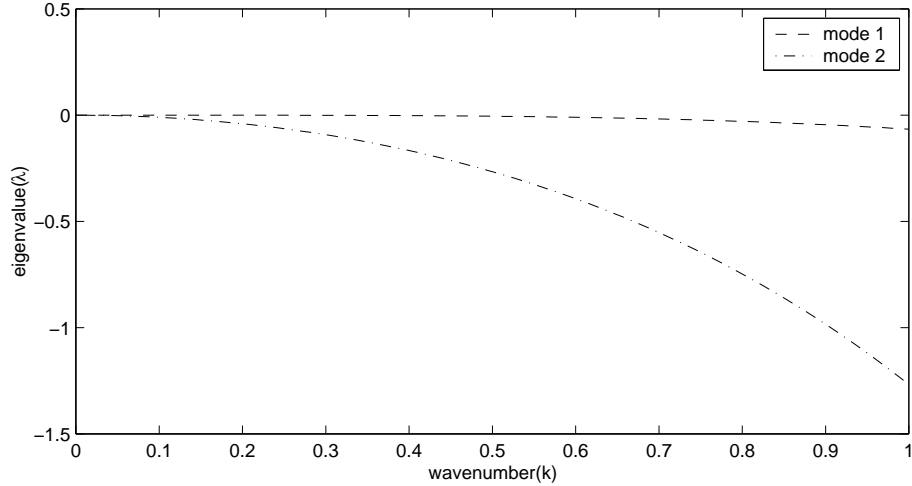


Figure 1: The eigenvalues of the linear modes (30) are plotted against the wavenumber  $k$ . This shows one mode decaying rapidly and one mode decaying very slowly. This slowly decaying mode represents physically long lasting corrugations on the surface maintained by in phase surfactant variations. The inverse Péclet number ( $\delta_s = 1/\mathcal{P}$ ) chosen here is the typical value  $10^{-4}$ .

dynamics of the system by perturbing these values. We assume a solution of these equations with initial sinusoidal ripples with growth rate  $\lambda$  or decay rate  $-\lambda$  and lateral wavelength  $k$  of the form

$$\eta = 1 + ae^{(\lambda t + ikx)} \quad \text{and} \quad \Gamma = 1 + be^{(\lambda t + ikx)} \quad (30)$$

for some  $a, b$ .

Substitute these expressions into the model (26–27) and neglect all non-linear terms in  $a$  and  $b$  to produce

$$\left(\lambda + \frac{k^4}{3}\right) a = -\left(\frac{k^2}{2}\right) b, \quad (31)$$

$$\left(\lambda + \delta_s k^2 + k^2\right) b = -\left(\frac{k^4}{2}\right) a. \quad (32)$$

Nontrivial solutions only exist when

$$\lambda^2 + \left(k^2 + \delta_s k^2 + \frac{1}{3}k^4\right) \lambda + \frac{1}{12}k^6 + \frac{1}{3}\delta_s k^6 = 0. \quad (33)$$

The eigenvalues of the linear modes (30),

$$\lambda = -\left(\frac{1}{2} + \frac{1}{2}\delta_s + \frac{1}{6}k^2\right) k^2$$

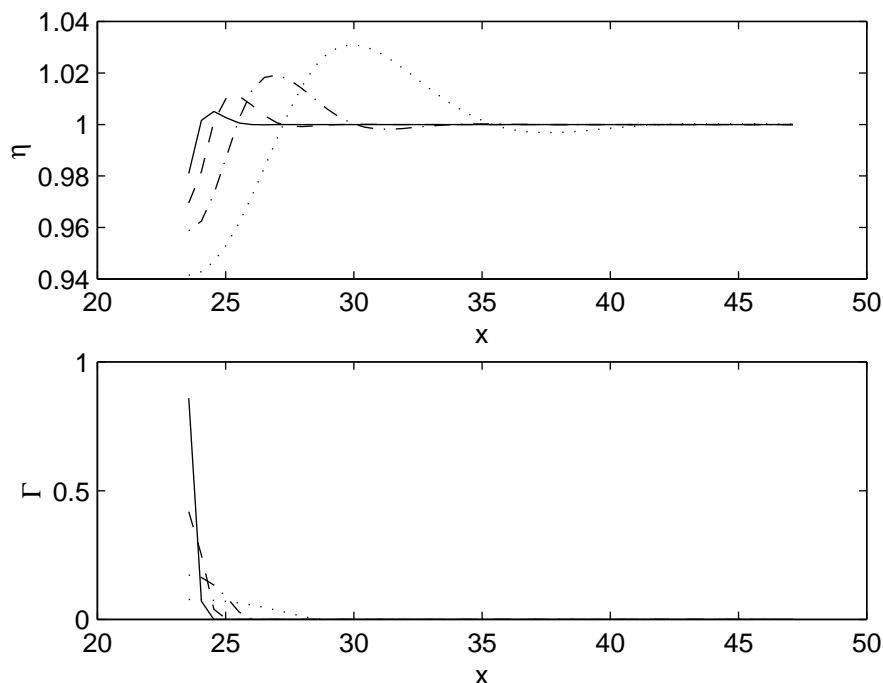


Figure 2: The film thickness (top) and surfactant concentration (bottom) profiles at non-dimensional times of  $t = 1$  (—),  $t = 10$  (- -),  $t = 100$  (-·-) and  $t = 1000$  (···). The initial conditions are a flat free surface with a drop of surfactant placed at  $x = 15\pi/2$ . Symmetry is assumed.

$$\pm \sqrt{\frac{1}{4}k^4 + \frac{1}{2}\delta_s k^4 + \frac{1}{12}k^6 + \frac{1}{4}\delta_s^2 k^4 - \frac{1}{6}\delta_s k^6 + \frac{1}{36}k^8}, \quad (34)$$

are plotted in Figure 1. They show that one mode decays rapidly with respect to the other which decays very slowly. This last mode denotes physically long lasting corrugations on the surface maintained by in phase surfactant variations.

This linear analysis of the dynamical system shows that the model is stable for all wave numbers  $k$ . Therefore the model (26–27) is structurally stable.

## 6 Numerical simulations

Our model (26–27) and the de Wit model (28–29) are solved for  $\eta(x, t)$  and  $\Gamma(x, t)$  using a standard 1<sup>st</sup> order backward time and 2<sup>nd</sup> order centred spatial

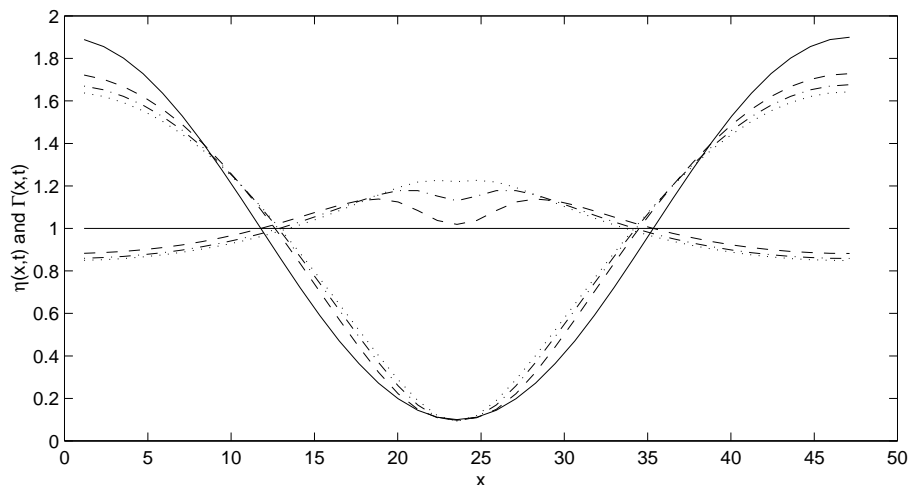


Figure 3: The film thickness (top) and surfactant concentration (bottom) profiles at non-dimensional times of  $t = 0$  (—),  $t = 15$  (- -),  $t = 30$  (-·-) and  $t = 45$  (···). The initial conditions are a corrugated free surface with a even layer of surfactant on the fluid.

differencing [5]. The properties of the fluid are taken to be surface tension  $\gamma = 30$  dynes/cm, viscosity  $\mu = 10^{-2}$  g/(cm s), density  $\rho = 1$  g/cm<sup>3</sup> and the surface diffusivity constant  $D_s = 10^{-4}$  cm<sup>2</sup>/s with the uniform thickness of the film  $10^{-5}$  cm and a drop of surfactant of  $10^{-10}$  mol/cm<sup>2</sup> placed initially in the centre of the fluid surface. This corresponds to a Reynolds number of  $\mathcal{R} = 3$ , a Bond number of  $\mathcal{B} = 3 \times 10^{-11}$ , a Hamaker constant of  $\mathcal{H} = 0.001$  and a Péclet number of  $\mathcal{P} = 1/\delta_s = 300$ . Therefore it is expected that the flow will be dominated by viscous forces and that the transport of surfactant will be dominated by advection.

For simulation over a large spatial domain, convergence was obtained with a single Newton step with a non-dimensional time step of  $\delta t = 100$  was on a spatial grid of  $N = 97$  points. This numerical scheme is stable for all time-steps (except when ludicrously big) and spatial grids. The time step of 100 is small enough so that the dynamics of a reasonable number of spatial modes are modelled accurately by the scheme.

Figure 2 shows the temporal evolution of the film thickness and surfactant concentration for our centre manifold model (26–27). The first graph plots  $\eta$ , the film thickness, as a function of  $x$  for various times whilst the second graph plots  $\Gamma$ , the surfactant concentration, also as a function of  $x$  for various times. Surface tension gradients formed due to the action of the surfactant result in the propagation of a front. The initially steep concentration gradients die

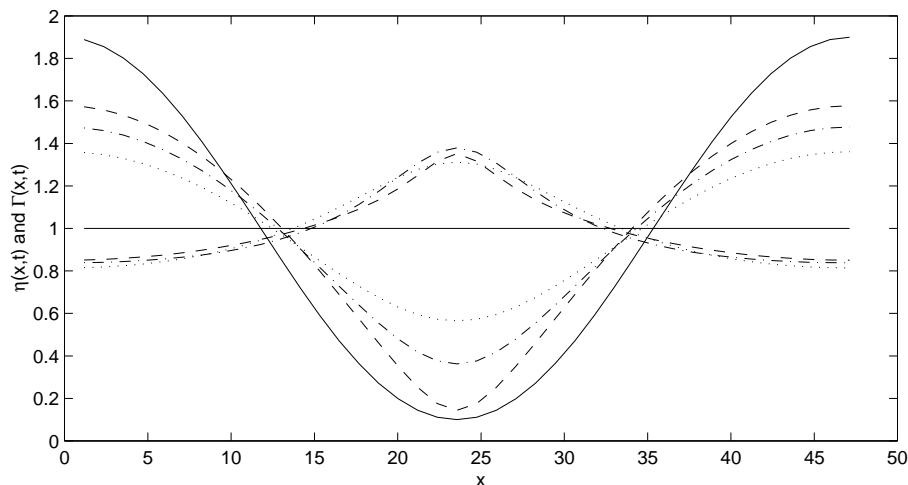


Figure 4: The film thickness (top) and surfactant concentration (bottom) profiles at non-dimensional times of  $t = 0$  (—),  $t = 100$  (- -),  $t = 200$  (-·) and  $t = 300$  (···). The initial conditions are a corrugated free surface with an even layer of surfactant on the fluid.

out over time due to the advection of the surfactant by the front.

The stability analysis in §5 shows that there could be long lasting corrugations on the surface maintained by in phase surfactant variations. Figures 3 and 4 show plots of the evolution of a fluid with an initially corrugated free surface contaminated with an even layer of surfactant. The initial deformation in Figure 3 shows the accumulation of surfactant in the trough caused by the pressure gradients driving fluid into the trough. After a non-dimensional time step of  $t = 45$  the raised concentration of surfactant generates surface tension gradients to oppose this collapse and leads to the corrugations lasting a long time as shown in Figure 3. This agrees with the stability analysis in Section 5 and demonstrates that surfactants hinder the levelling of thin films.

Our model for the temporal surfactant evolution (27) when compared with the de Wit model, contains additional fourth order terms involving  $\eta_x^2$ . The enhanced accuracy of the model becomes apparent when the surface gradients,  $\eta_x$ , are sufficiently large. Figure 5 shows a comparison between our model and the de Wit model. The difference between the two solutions is plotted at a common nondimensional time of  $t = 10$  and shows the increasing disparity as the Péclet number is decreased.

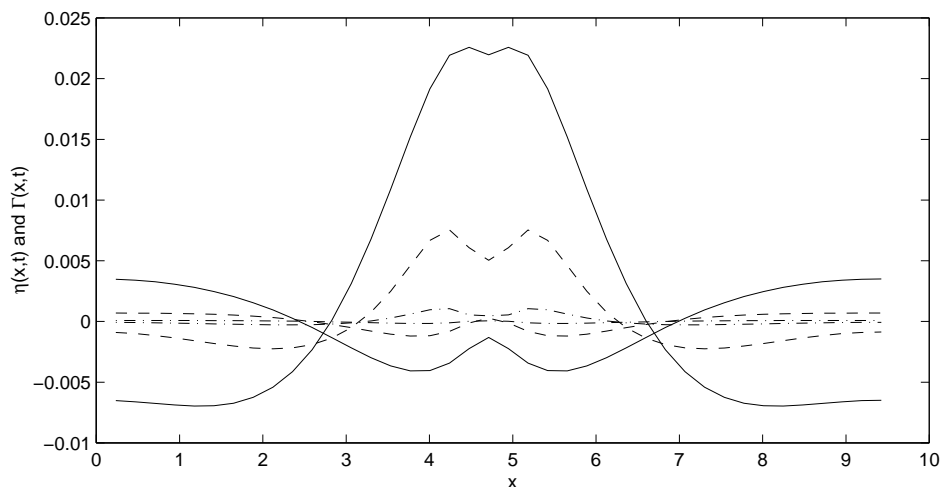


Figure 5: The film thickness (top) and surfactant concentration (bottom) profiles at the same nondimensional time,  $t = 10$ . The graphs plot the difference between the centre manifold model, (26–27), and the de Wit model (28–29), at different Péclet numbers  $\mathcal{P} = 3$  (—),  $\mathcal{P} = 30$  (- -) and  $\mathcal{P} = 300$  (-·-). As the Péclet numbers decrease the difference between the models increase.

## 7 Summary

In this paper we have developed a comprehensive structurally stable model of the dynamics of the spreading of a contaminant on a thin fluid. The centre manifold approach we adopt incorporates all the physical effects at the appropriate stage in the modelling. Numerical simulations have demonstrated the importance of the extra terms in our model compared with other models developed using other methods.

## References

- [1] A.W. Adamson. *Physical Chemistry of Surfaces*. Wiley Interscience, 1967.
- [2] J. Ahmad and R.S. Hansen. A simple quantitative treatment of the spreading of monolayers on thin liquid films. *J. Colloid Interface Sci.*, 38:601–604, 1988.

- [3] J. Carr. Applications of centre manifold theory. In *Vol. 35, Applied Math. Sci.* Springer–Verlag, 1981.
- [4] A. De Wit, D. Gallez, and C.I. Christov. Nonlinear evolution equations for thin liquid films with insoluble surfactants. *Phys. Fluids*, 6:3256–3266, 1994.
- [5] G. Degrez. Implicit time-dependent methods for inviscid compressible flows, with a discussion of the concept of numerical dissipation. In Wendt J.F., editor, *Computational Fluid Dynamics: An Introduction*. Springer-Verlag, 1992.
- [6] N.D. DiPietro and R.G. Cox. The containment of an oil slick by a boom placed across a uniform stream. *J. Fluid Mech.*, 96:613–640, 1980.
- [7] N.D. DiPietro, C. Huh, and R.G. Cox. The hydrodynamics of the spreading of one liquid on the surface of another. *J. Fluid Mech.*, 84:529–549, 1978.
- [8] M. Foda and R.G. Cox. The spreading of thin liquid films on a water–air interface. *J. Fluid Mech.*, 101:33–51, 1980.
- [9] Th. Gallay. A center-stable manifold theorem for differential equations in banach spaces. *Commun. Math. Phys.*, 152:249–268, 1993.
- [10] D.P. Gaver III and J.B. Grotberg. The dynamics of a localized surfactant on a thin film. *J. Fluid Mech.*, 213:127–148, 1990.
- [11] H. Haken. *Synergetics, An Introduction*. Springer–Verlag, 1993.
- [12] M. Hărăgus. Model equations for water flow in the presence of surface tension. *preprint*, 1995.
- [13] Z. Hussain, M. Fatima, and J. Ahmad. The rate of spreading of monolayers on liquids. *J. Colloid Interface Sc.*, 50:44–48, 1975.
- [14] D.B.R. Kenning. Two-phase flow with nonuniform surface tension. *App. Mechs. Rev.*, 21(1):1101–1111, 1968.
- [15] V.G. Levich. *Physicochemical Hydrodynamics*. Prentice–Hall, 1962.
- [16] C. Maldarelli, R.K. Jain, I.V. Ivanov, and E. Ruckenstein. Stability of symmetric and unsymmetric thin liquid films to short and long wavelength perturbations. *J. Colloid Interface. Sci.*, 78:118–143, 1980.



- [17] A.J. Roberts. The application of centre manifold theory to the evolution of systems which vary slowly in space. *J. Austral Math. Soc. B*, 29:280–300, 1988.
- [18] A.J. Roberts. Low-dimensional models of thin film fluid dynamics. *Phys. Letters A*, 212:63–71, 1996.
- [19] A.J. Roberts. Low-dimensional modelling of dynamics via computer algebra. *Comp. Phys. Comm.*, 100:215–230, 1997.
- [20] R. Valéry Roy, A.J. Roberts, and M.E. Simpson. A lubrication model of coating flows over a curved substrate in space. *Technical report*, [<http://arXiv.org/abs/patt-sol/9705002>], *submitted to J Fluid Mech*, 1997.
- [21] L.W. Schwartz and D.E. Weidner. Modeling of coating flows on curved surfaces. *J. Engrg. Math.*, 29:91–103, 1995.
- [22] A. Sheludko. Thin liquid films. *Adv. Colloid Interface Sc.*, 1:392–464, 1967.
- [23] C-S. Yih. Fluid motion induced by surface-tension variation. *Phys. Fluids*, 11:477–480, 1968.

## A Computer algebra code

A computer algebra program to perform all the necessary detailed algebra for this physical problem was used. An important feature of this iteration is that it is performed until the residuals of the actual governing equations are zero, to some order of error. Thus the correctness of the results is based only upon the correct evaluation of the residuals and sufficient iterations.

```

1   % Construct slowly-varying centre manifold of 2D thin film
2   % fluids. Allows for large changes in film thickness.
3   % Allows for surfactants, inertia and van der Waal forces.
4   %
5   on div; off allfac; on revpri; factor d; % improves printing
6   % use stretched coordinates: ys=y/h(x,t), xs=x, ts=t
7   % adapted by M.E. Simpson (1996) from a program written
8   % by A.J. Roberts

```

```

9   depend xs,x,y,t;
10  depend ys,x,y,t;
11  depend ts,x,y,t;
12  let { df(~a,x) => df(a,xs)-ys*h(1)/h(0)*df(a,ys)
13        , df(~a,t) => df(a,ts)-ys*g/h(0)*df(a,ys)
14        , df(~a,y) => df(a,ys)/h(0)
15        , df(~a,x,2) => df(df(a,x),x) };
16  % solves -df(p,ys)=rhs s.t. sub(ys=1,p)=0
17  operator psolv; linear psolv;
18  let {psolv(ys^n,ys) => (1-ys^(n+1))/(n+1)
19        ,psolv(ys,ys) => (1-ys^2)/2
20        ,psolv(1,ys) => (1-ys) };
21  % solves df(u,ys,2)=rhs s.t. sub(ys=0,u)=0
22  % & sub(ys=1,df(u,y))=0
23  operator usolv; linear usolv;
24  let {usolv(ys^n,ys) => (ys^(n+2)/(n+2)-ys)/(n+1)
25        ,usolv(ys,ys) => (ys^3/3-ys)/2
26        ,usolv(1,ys) => (ys^2/2-ys) };
27  % use operator h(m) to denote df(h,x,m)
28  operator h;
29  depend h,xs,ts;
30  let { df(h(~m),xs) => h(m+1)
31        ,df(h(~m),xs,2) => h(m+2)
32        ,df(h(~m),ts) => df(g,xs,m) };
33  % use operator c(m) to denote df(c,x,m)
34  operator c;
35  depend c,xs,ts;
36  let { df(c(~m),xs) => c(m+1)
37        ,df(c(~m),xs,2) => c(m+2)
38        ,df(c(~m),ts) => df(f,xs,m) };
39  depend gam,xs;
40  gam := g0 + con*(1-c(0));
41  %
42  % linear solution
43  u:=0; v:=0; p:=0; g:=0; f:=0;
44  %
45  % Iteration. Use d to count the number of derivatives
46  % of x, and throw away this order or higher in d/dx
47  %let {d^5=0,con^2=0};
48  con:=cn*d^2;
49  ham:=hm*d^2;

```

```

50  b:=bb*d^2;
51  let d^5=0;
52  curv:=1-h(1)^2*d^2/2+3*h(1)^4*d^4/8-5*h(1)^6*d^6/16;
53  scal:=1+h(1)^2*d^2/2-h(1)^4*d^4/8+h(1)^6*d^6/16;
54  repeat begin
55    % continuity & bed
56    write ceq:=-df(u,x)*d-df(v,y);
57    v:=v+h(0)*int(ceq,ys);
58    % vertical momentum & normal stress
59    write veq:=re*( df(v,t)+u*df(v,x)*d+v*df(v,y) )
60                  +df(p,y) -df(v,x,2)*d^2-df(v,y,2) +b;
61    write tn:= sub(ys=1,-p*(1+h(1)^2*d^2)
62                +2*(df(v,y)+h(1)^2*d^3*df(u,x)
63                  -h(1)*d*(df(u,y)+df(v,x)*d))
64                -gam*df(h(1)*d*curv,x)*d*(1+h(1)^2*d^2) );
65    p:=p+h(0)*psolv(veq,ys) +tn;
66    % horizontal momentum & bed & tangential stress
67    write ueq:=re*( df(u,t)+u*df(u,x)*d+v*df(u,y) )
68                  +df(p,x)*d -df(u,x,2)*d^2-df(u,y,2)
69                  -3*ham*df(h(0),x)*d/h(0)^4;
70    write tt:=-sub(ys=1, (1-d^2*h(1)^2)*(df(u,y)+df(v,x)*d)
71                  +2*h(1)*d*(df(v,y)-df(u,x)*d)
72                  -curv*df(gam,x)*d*(1+h(1)^2*d^2) );
73    u:=u+h(0)^2*usolv(ueq,ys)+h(0)*tt*ys;
74    g:=sub(ys=1,v-u*h(1)*d);
75    f:=-curv*(c(0)*h(1)*d*df(g,x)*d*curv
76          -df(db*c(1)*d*curv^2,x)
77          *d+df(c(0)*sub(ys=1,u)*scal,x)*d);
78  end until (veq=0)and(tn=0)and(ueq=0)and(tt=0)and(ceq=0);
79  ;end;

```